Adsorption of Block-Copolymer Micelles from a Selective Solvent

J. C. Meiners, A. Quintel-Ritzi,† and J. Mlynek

Fakultät für Physik, Universität Konstanz, Postfach 5560, D-78434 Konstanz, Germany

H. Elbs and G. Krausch*

Institut für Physikalische Chemie, LMU München Theresienstrasse 39, D-80333 München, Germany

Received March 11, 1997[⊗]

ABSTRACT: We have studied the adsorption of poly(styrene-*b*-2-vinylpyridine) block copolymers from a selective solvent onto a flat solid substrate, resulting in the formation of laterally ordered microdomains. We address the question whether the lateral domain structure is due to adsorption of entire micelles from the solution. Dynamic light scattering, atomic force microscopy, surface plasmon spectroscopy, and transmission electron microscopy were used to characterize the polymer solution, the adsorption process, and the resulting polymer layer, respectively. A quantitative comparison of the results obtained with different techniques strongly indicates direct adsorption of whole micelles onto a brush formed from free copolymer chains. Furthermore, the adsorption process is found to depend strongly on the velocity at which the samples are withdrawn from the solution.

I. Introduction

The microdomain structure in thin films of diblock copolymers has been extensively studied in recent years. In the melt, one generally observes accumulation of one of the blocks at each boundary surface of the film, since the reduction in interfacial energy related to this accumulation will lower the overall free energy of the system.[1] For thin films of symmetric diblock copolymers, the formation of surface-induced, highly ordered multilayers of microdomains is now well established.[2] With asymmetric diblock copolymers, the situation is somewhat more complex and experimental data are rare. However, at least close to the boundary surfaces, preferential accumulation of one of the blocks has also been observed.[3,4] In the presence of laterally homogeneous boundary surfaces, the surface effects generally lead to a laterally homogeneous distribution of polymer, and the formation of ordered *lateral* structures in thermodynamic equilibrium is difficult to obtain. Only recently, Spatz *et al.*[5] demonstrated a laterally ordered equilibrium microdomain structure in an ultrathin film of a symmetric P(S-*b*-2VP) diblock copolymer on a mica surface. For lateral microphase separation to occur it proved essential that the film thickness was kept much smaller than the thickness of a complete lamella.

While laterally ordered microdomain structures in thin polymer films are only rarely found in the thermal equilibrium of the melt, different routes can be taken to obtain such structures far from the melt equilibrium situation. It has been shown that under suitable conditions, the adsorption of diblock copolymers from a selective solvent followed by rapid solvent extraction can lead to highly ordered lateral microdomains.[6−11] Atomic force microscopy (AFM) and transmission electron microscopy (TEM) have been used to show that the individual structures consist of a core of the insoluble block surrounded by a highly stretched corona of the soluble block. Such structures, an example of which is shown in Figure 1, are produced via a quite simple experimental route, i.e., by dipping a smooth, clean substrate into the polymer solution and letting it dry.

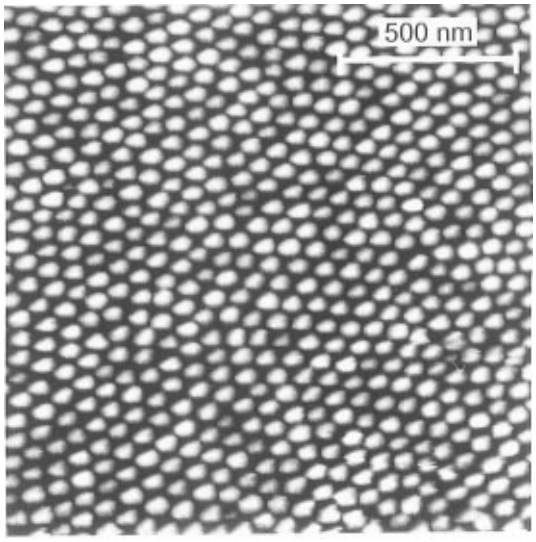

Figure 1. AFM image showing the topography of a P(S-*b*-2VP) micelle film on a mica surface, prepared from a 3 mg/mL solution of a symmetric diblock copolymer ($M_{W(PS)}/M_{W(PVP)}$ = 84K/91K) in toluene. The gray scale indicates the height of the micellar structure ranging from 0 (black) to 30 nm (white).

While the formation of such structures has been established by various authors and has been used to create, e.g., ordered arrays of metal nanoparticles,[9] the details of the formation process are still under contention. This holds in particular for the formation of lateral microdomains in pure diblock copolymers, i.e., without further stabilization of polymeric micelles through ionic complexation in solution. Although the adsorption process has never been looked at in detail, most of the experimental studies assume that the surface structures result from the adsorption of entire micelles, which collapse onto the substrate surface after solvent evaporation.[8] Li *et al.* on the other hand recently suggested that the observed structures are due to a particular equilibrium structure of a concentrated copolymer solution near an attractive wall.[11] In the present paper, we concentrate on the adsorption process for P(S-*b*-2VP) diblock copolymers from toluene solution onto mica

† Present address: Universität Bern; Dept. f. Chemie u. Biochemie, Freiestr. 3 - CH-3012, Bern, Germany.

* Corresponding author. Tel: +49-89-2394-4515. Fax: +49-89-2805-248. E-Mail: georg.krausch@lrz.uni-muenchen.de.

⊗ Abstract published in *Advance ACS Abstracts,* July 15, 1997.

S0024-9297(97)00327-6 CCC: $14.00

surfaces and try to distinguish between the two possible scenarios. We shall give strong experimental evidence for the adsorption of entire micelles.

The paper is organized as follows. After a short Experimental Section, we try to analyze the different stages of structure formation. The micellar solution is characterized by dynamic light scattering in order to obtain the critical micelle concentration, the hydrodynamic radius of the micelles, and their aggregation number. The latter two numbers are compared to the results of AFM measurements performed after solvent extraction. The adsorption process is followed in situ via surface plasmon spectroscopy in solution and after solvent extraction in order to find at what stage of the adsorption process the surface structure is formed. Thereafter, adsorption from mixtures of pure polymer micelles and $CoCl_2$-labeled polymer micelles are investigated. The results strongly indicate that entire micelles are adsorbed. Finally, we investigate the role of the velocity at which the samples are withdrawn from solution. The results are then discussed in view of the earlier work quoted above.

II. Experimental Section

In our study, a symmetric and an asymmetric poly(styrene)−poly(2-vinylpyridine) (P(S-*b*-2VP)) block copolymer have been used. The materials have been polymerized via anionic polymerization.[12] The molecular weights were $M_{W(PS)}/M_{W(PVP)}$ = 84K/91K for the symmetric and $M_{W(PS)}/M_{W(PVP)}$ = 20K/120K for the asymmetric block copolymer corresponding to indices of polymerization of N_{PS}/N_{PVP} = 800/870 and N_{PS}/N_{PVP} = 190/1145, respectively. Both polymers were dissolved in toluene, which acts as a selective solvent for PS. The selectivity of the solvent gives rise to the formation of micelles in such a solution, if the concentration exceeds a certain critical micelle concentration (cmc). As substrates, freshly cleaved sheets of mica have been used. For the TEM studies, TEM copper grids coated with thin films of carbon were used.

For the adsorption experiments, all substrates were dipped into the polymer solution for about 20 s, withdrawn from solution, and dried in air at room temperature. Details of this procedure have been reported elsewhere.[6] The velocity at which the samples were taken out of the solution was controlled by a motor and could be varied between 0.3 and 3.5 mm/s. The polymer concentration was varied between 0.001 and 12 mg/mL.

To obtain the surface topography after drying, the samples were imaged with a commercial atomic force microscope both in contact mode and in tapping mode. Care was taken not to destroy the polymer microstructures during imaging. Some of the samples were imaged with transmission electron microscopy by using a Zeiss EM 900 microscope operated at 50 kV.

To characterize the properties of the solution prior to polymer adsorption, dynamic light scattering was used. The solution was illuminated at λ = 488 nm (Spectra 2025 Ar^+-ion laser) in a cuevette kept at a constant temperature of 294 K. The autocorrelation function was recorded at different scattering angles. From the first moment of the correlation function, the translational diffusion coefficient is calculated, which in turn yields the hydrodynamic radius of the aggregates in solution via the Einstein−Stokes relation.

In order to follow the adsorption of polymer in situ, the resonance angle for excitation of surface plasmons at the interface between a thin metal film and the polymer solution was determined. A flint glass prism coated with a 53-nm-thick layer of silver was placed in a cuevette. From the outside, two p-polarized laser beams at λ = 632.8 nm (HeNe laser) were coupled into the prism such that they were totally reflected from the silver film. Both beams were convergent and thus covered a range of angles of incidence. Depending on the boundary conditions at the silver film, which are determined by the refractive index of the surrounding medium, surface plasma oscillations can be excited only under a particular angle of incidence. If such a resonant plasmon excitation occurs, energy is transferred from the laser beam to the plasmon and the reflection from the silver film is attenuated under that resonance angle. We aligned both laser beams such that their center angle of incidence corresponds to the resonance angle for a surface plasmon excitation in the silver film without polymer coverage in air and toluene, respectively. The extinction of the beams was monitored with movable photo diodes. Thus a shift in the resonance angle upon adsorption of the polymer is conveniently measured. From the shift of the resonance angle, the amount of adsorbed polymer can be calculated.

III. Results

III.1. Atomic Force Microscopy. Figure 1 shows an AFM image revealing the topography of a P(S-*b*-2VP) film adsorbed onto a mica surface from a solution at a concentration of 3 mg/mL at room temperature. Additional TEM studies show that the topography corresponds to a microdomain structure with isolated PVP cores located in the center of the protrusions. The PVP cores are embedded into a PS matrix. While the resulting structures have been discussed in detail in earlier publications,[6,10] here we utilize the AFM image for a quantitative estimate of the aggregation number of the individual microdomains.

For the symmetric copolymer (N_{PS}/N_{PVP} = 800/870) we find an average nearest neighbor distance between the protrusions of 82 ± 5 nm with a typical height of 15 ± 2 nm.[13] We model the aggregates as spherical caps of height 15 nm and diameter 82 nm, resulting in a volume of 4.1×10^{-17} cm^3 per microdomain. Assuming an average bulk density of 1.1 g/cm^3, an aggregation number of $p \cong 155$ chains per microdomain is found. For the asymmetric copolymer, a similar calculation yields $p \cong 358$.

It is instructive to quantitatively estimate the uncertainty of these numbers. In the spherical cap approximation, the experimental errors stated above for the diameter and the height of the microdomains result in a 28% error for the determination of their volume. In addition, the density of the thin polymer film may well deviate from the bulk density of the same material. Lacking any data on this effect, we may estimate a 10% uncertainty of the density. This rather conservative assumption leads to $p \cong 155 \pm 48$ chains per microdomain for the symmetric block copolymer. For the asymmetric copolymer, one finds $p \cong 358 \pm 107$.

III.2. Dynamic Light Scattering. In a second step, we will now discuss the properties of the block copolymer solution. In order to determine the critical micelle concentration and to measure the size of the micelles, we have performed dynamic light scattering on solutions of both block copolymers at various concentrations. This technique yields the diffusion coefficient D_0 of the polymer aggregates in the solution, and thus via the Stokes−Einstein relation

$$R = \frac{k_B T}{6\pi\eta D_0} \tag{1}$$

the hydrodynamic radius R of the aggregates, with η being the viscosity of the solvent. The results are shown in Figure 2 for the symmetric copolymer. We find that the radii of the polymer aggregates rise sharply for both polymers at a concentration of about 0.03 mg/mL, which we identify as the critical micelle concentration (cmc) of the solutions. This value is in fair agreement with

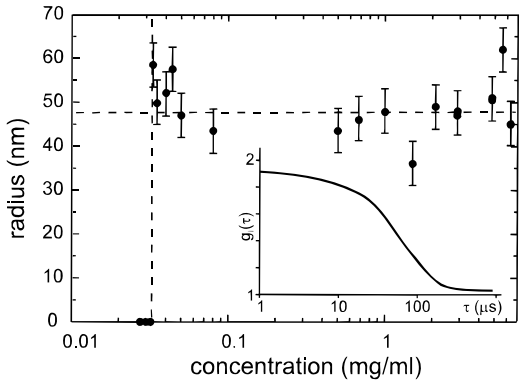

Figure 2. Radius of P(S-*b*-2VP) ($M_{W(PS)}/M_{W(PVP)}$ = 84K/91K) aggregates in toluene, as determined by means of dynamic light scattering. The inset shows a typical intensity autocorrelation function $g_I(\tau)$ recorded at a scattering angle of 70°.

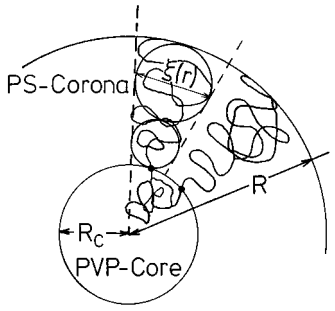

Figure 3. Model of micelles with a PVP core and a PS corona in a selective solvent in the Daoud−Cotton blob model.[10,11] R denotes the radius of the micelle, R_C the radius of the core, and $\xi(r)$ the size of a blob.

the results reported by Tassin *et al.* for similar systems.[14] Above the cmc, we find a hydrodynamic radius of 48 ± 8 nm for the symmetric block copolymer. Within the experimental uncertainties, the hydrodynamic radius is found to be independent of polymer concentration.

Above the cmc, the number of chains per micelle p can be estimated from the radius R of the micelles. For this aim, a simple model for the micelle is used. Following the notion of Marques *et al.*,[15] the micelle is regarded as a spherical molten core of the insoluble PVP block, surrounded by a swollen PS corona. The radius of the core R_C is given by

$$R_C = \left(\frac{3}{4\pi} p N_{PVP}\right)^{1/3} a \tag{2}$$

with a being a statistical segment length of PVP. A corona of PS chains is grafted to this core with the junction points of the block copolymers located at the core surface as sketched in Figure 3. Having p polymer chains in each micelle, the junction points have a normalized surface density σ on the surface of the PVP core,

$$\sigma = \frac{p a^2}{4\pi R_C^{\,2}} \tag{3}$$

with an average distance $d = a\sigma^{-1/2}$ between them.

Polymer layers grafted to a sphere have been studied by Daoud *et al.*,[16,17] originally for star-shaped polymers, later by Bug *et al.*[18] for micelles of polymeric surfactants, and eventually for block copolymer micelles by Marques *et al.*[15] They introduced the notion of polymer blobs which describe the local polymer distribution in the corona. Each of the blobs is characterized by a diameter $\xi(r)$, which increases with the distance r from the center of the micelle

$$\xi(r) = \frac{d}{R_C} r \tag{4}$$

In the corona, the PS is in a good solvent, and therefore its distribution is governed by excluded-volume statistics. Thus a blob of size $\xi(r)$ contains

$$g(r) = \left(\frac{\xi(r)}{a}\right)^{5/3} \tag{5}$$

monomers, and the local monomer concentration $c(r)$ is given by

$$c(r) = \frac{6g(r)}{\pi \xi^3(r)} = \frac{6}{4^{2/3}} \pi^{-5/3} r^{-4/3} p^{2/3} a^{-5/3} \tag{6}$$

Integration over the entire corona volume yields the total number of PS monomers:

$$N_{PS} p = \int_{R_C}^{R} 4\pi r^2 c(r)\, \mathrm{d}r \tag{7}$$

Hence we find for the micellar radius

$$R = a\left(\frac{5}{18} 4^{-1/3} \pi^{2/3} p^{1/3} N_{PS} + 3^{5/9} (4\pi)^{-5/9} p^{5/9} N_{PVP}^{\;5/9}\right)^{3/5} \tag{8}$$

With the dynamic light scattering data shown above and the known degrees of polymerization, we find an aggregation number p = 113 for the symmetric block copolymer. This number is in fair agreement with the aggregation number estimated from the size of the microdomains imaged with AFM. In addition, the hydrodynamic radius R = 48 ± 8 nm observed in solution is in good agreement with the radius R = 41 ± 3 nm as determined with AFM for the adsorbed aggregates.

For the asymmetric copolymer the situation is similar. However, the aggregation number determined from the light scattering data turns out to be somewhat too large as compared to the estimate revealed from the AFM experiments. We note that for the PVP-rich asymmetric copolymer the hydrodynamic radius strongly depends on the exponent used in eq 2 to describe the chain conformation in the PVP core. If, instead of an entirely molten core, some penetration of the solvent into the core is assumed, a slightly higher exponent is expected. However, changing the exponent from 1/3 to say 0.36 already leads to a significant reduction in the aggregation number and removes the discrepancy between the light scattering and AFM data. We have checked the swelling behavior of PVP in toluene qualitatively by measuring the thickness change of a thin PVP film after exposure to toluene vapor. Indeed, the film thickness was found to increase slightly, supporting the above argument. We note that the numbers determined in the present study are consistent with aggregation numbers estimated for other block copolymer systems.[19−21]

A critical inspection of the errors involved in determining the aggregation numbers both by AFM and by light scattering shows that care has to be taken before drawing an ultimate conclusion from the experimental evidence discussed so far. For the present, we only note

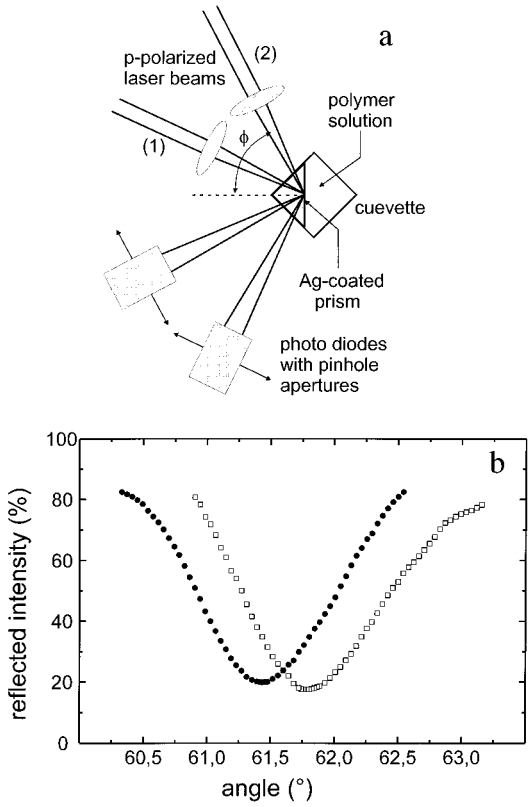

Figure 4. (a) Experimental setup for the surface plasmon resonance measurement. (b) Plasmon resonance curves in pure toluene (●) and in a 3 mg/mL solution of P(S-*b*-2VP) ($M_{W(PS)}/M_{W(PVP)}$ = 20K/120K) in toluene (○).

that the experimental data are in agreement with the notion of entire micelles adsorbing onto the substrates without any surface induced rearrangement of chains. We shall present more direct evidence for the notion of entire micelle adsorption in section III.4 of this paper.

III.3. Surface Plasmon Spectroscopy. We now turn to the direct adsorption of the polymer chains when the substrate is immersed into the solution. AFM images of the adsorbate films on polar substrates such as mica already indicate that there is a laterally homogeneous polymer film adsorbed underneath the micelles.[6] It has been demonstrated that for polymer concentrations around the cmc only few isolated protrusions on an otherwise homogeneous polymer film are found after adsorption. The thickness of the film between the protrusions was determined to be about 4 nm. Thus it was conjectured that this thin film is a collapsed copolymer brush formed by the adsorption of free chains. The PVP block acts as an anchor, while the PS blocks are swollen in the solvent. On solvent extraction, the brush collapses. It was assumed that at higher copolymer concentrations, additional copolymer is adsorbed on top of this brush surface. This notion was confirmed by various other experiments.[8,11]

In order to get experimental access to the adsorption process itself, we have measured the amount of polymer adsorbed in solution and in air by means of surface plasmon spectroscopy.[21] Although this method does not provide any lateral information, it is well suited for an *in-situ* measurement of the thickness of block copolymer layers in solution. In principle, our measurement closely follows the method described by Tassin *et al.*,[14] although we used a somewhat simpler experimental setup (Figure 4a). Since the excitation of surface plasmons in a total internal reflection setup requires a metal coated surface, we first had to assure that the microdomain structures formed on mica could be reproduced on thin silver films as well. This is indeed the case. As a matter of fact, we could image the Ag-coated flint glass prisms used for the surface plasmon measurements by AFM after solvent extraction and found microdomain structures closely resembling the data shown in Figure 1.

Table 1. Adsorbed Brush in Solution. Calculated Thickness of the Collapsed PVP Layer d_{PVP}, the Swollen PS Brush d_{PS}, and the Resulting Shift of the Surface Plasmon Resonance Angle $\Delta\phi_{calcd}$, Compared to the Measured Shift in the Resonance Angle $\Delta\phi_{exptl}$

$M_{W(PS)}/M_{W(PVP)}$	d_{PVP}, nm	d_{PS}, nm	$\Delta\phi_{calcd}$	$\Delta\phi_{exptl}$
84K/91K	1.2	78.5	0.35°	0.30°
20K/120K	1.9	19.5	0.22°	0.25°

We first determined the surface plasmon resonance angle of the silver film in air. Then the cuevette was filled with toluene, and the resonance angle in this environment was measured. Subsequently, some concentrated block copolymer solution is added to the toluene. Within a few seconds, the resonance angle was found to shift toward larger values indicating some copolymer adsorption at the silver surface. After equilibrium was reached, the polymer solution was quickly removed from the cuevette with a pipette. After the adsorbate film had dried, the resonance angle was measured again. Finally, the prism was removed from the cuevette and the adsorbate film on the silver surface was imaged with a stand-alone AFM.[22] In all instances, micellar surface structures as previously discussed were found.

As an example, Figure 4b shows surface plasmon resonances in toluene before and after addition of the copolymer. Addition of the copolymer leads to a shift of the resonance angles of $\Delta\Phi = 0.35°$ and $\Delta\Phi = 0.22°$ for the symmetric and the asymmetric copolymers, respectively. We can compare the measured values with calculated ones, assuming different adsorption scenarios. Assuming that only a polymer brush is adsorbed in solution, one can model the adsorbed layer as a bilayer consisting of a dense PVP layer adsorbed at the silver film and a swollen PS layer on top. We may use the AFM results quoted above and calculate the surface density of chains σ from the thickness of the homogeneous polymer layer adsorbed at low polymer concentrations.[28] From this number, the thickness d_{PS} of the swollen PS layer can be calculated according to Hadzioannou *et al.*:[23]

$$d_{PS} = N_{PS} a \sigma^{1/3} \tag{9}$$

Assuming that the PVP block forms a molten layer on the surface, with the swollen PS layer on top of it, the boundary conditions for the surface plasmon excitation in the polymer solution can be modeled. Equation 9 results in brush thicknesses of 78.5 and 21.5 nm for the symmetric and asymmetric copolymers, respectively. With the refractive indices $n = 1.57$ for PVP and $n = 1.50$ for the swollen PS layer, one can calculate the expected shift in the surface plasmon resonance angle. We note that for the PS layer, an average refractive index was used assuming a PS volume fraction of 0.1 in the brush. The results of these calculations are shown in Table 1 together with the experimental numbers and in fact suggest that only a brush is adsorbed. More importantly, these numbers are not consistent with the notion of micelles bound either to

Table 2. Shift of the Plasmon Resonance Angle from a Dry P(S-*b*-2VP) Adsorbate Film $\Delta\phi_{exptl}$ and Inferred Thickness of the Film $d_{P(S-b-2VP)}$

$M_{W(PS)}/M_{W(PVP)}$	$\Delta\phi_{exptl}$	$d_{P(S-b-2VP)}$, nm
84K/91K	2.2°	25
20K/120K	3.1°	29

the substrate or to the brush in this early stage of the adsorption process. This holds in particular for the asymmetric polymer: here the plasmon resonance data only allow for some 20 nm of swollen polymer, the micelles in solution, however, are of about 90 nm in diameter.

The surface plasmon data obtained at air after the polymer film has dried show that the film is thicker than the collapsed 4-nm brush. Modeling the polymer film as a homogeneous film with an average refractive index of 1.56, we find a thickness of 25 nm for the symmetric and 29 nm for the asymmetric block copolymer (Table 2). These findings are in agreement with subsequent AFM measurements on the adsorbate films, which show the typical micellar structure. Thus the adsorption process happens in two steps: First, the underlayer brush is adsorbed, then, when the substrate is removed from the solution, additional material is deposited on top of the brush.

III.4. Transmission Electron Microscopy. Given the results discussed above, there is strong evidence for the adsorption of entire micelles onto the block copolymer brush rather than a surface-driven rearrangement of chains after free chain adsorption. Aiming toward direct experimental evidence for micelle adsorption from solution, we made use of the relatively high stability of the micelles in solution, as opposed to the high mobility of free chains. Two micellar solutions of P(S-*b*-2VP) with $M_{W(PS)}/M_{W(PVP)}$ = 84K/91K at a concentration of 1.5 mg/mL were prepared in toluene. To one of these solutions, 0.5 mg/mL $CoCl_2$ was added. Transition metal salts are known to form intrachain complexes with isotactic poly(2-vinylpyridine), while interchain complexes as known for atactic poly(4-vinylpyridine) are considered impossible for steric reasons.[24] Therefore, in contrast to what would be expected for poly(4-vinylpyridine), the stability of the micelles is only insignificantly affected by complex formation.[25] The resulting solution should consist of $CoCl_2$-labeled P(S-*b*-2VP) micelles and free chains. This solution was subsequently mixed with the unlabeled polymer solution. Carbon-coated TEM grids where then dipped into the mixture of the two solutions at different times after mixing.

Since both the micelles and the free chains have a high mobility in the solution, labeled and unlabeled micelles and free chains mix quickly. In contrast, an exchange of polymer chains between different micelles is expected to take place on a much larger time scale. Hence, at short times after mixing, micelles are still either labeled or unlabeled, depending on which solution they stem from. At later times, the exchange of polymer chains between the micelles becomes effective, and eventually all micelles will exhibit roughly equal amounts of transition metal salt. Regarding the adsorption process, two scenarios can now be distinguished: If entire micelles are adsorbed, we expect a random mixture of labeled and unlabeled micelles on the surface for samples dipped into the mixed solution at early times after mixing. Samples dipped sufficiently late after mixing should then be homogeneously labeled with $CoCl_2$. If on the other hand a complex rearrangement of chains were responsible for the observed micellar structure at the surface, the resulting structure should be homogeneously labeled even at early times after the mixing.

Figure 5 shows the result of this experiment. On the sample dipped immediately after the two solutions were mixed, only some strongly labeled microdomains are visible (Figure 5a). On a sample dipped 2 min after mixing, however, we see a densely packed microdomain pattern in which some of the PVP domains appear with a strong contrast, while others appear weaker (Figure 5b). Eventually, after about 10 min, all micelles are visible with almost the same contrast (Figure 5c). This finding is easily understood given the assumption that entire micelles adsorb without further rearrangement of chains. At early times, the micelles originating from the unlabeled solution are not labeled at all and therefore cannot be observed with TEM. Consequently, only the micelles originating from the labeled solution are visible and appear as randomly distributed, isolated aggregates in Figure 5a. Some time after mixing the intermicellar chain exchange has lead to at least some labeling in the originally unlabeled micelles, which now appear weakly labeled in Figure 5b. Now the densely packed structure of the film is revealed. Sufficiently long times after mixing, the system has equilibrated in solution and all micelles are labeled to a similar extend. These findings are a strong indication for the adsorption of entire micelles onto the brush-coated substrate surface.

III.5. Effect of Drawing Velocity. The experimental evidence discussed so far shows that only a homogeneous brush is absorbed in solution onto a polar substrate, while an adsorbed layer of micelles is observed after removing the samples from solution and drying. Therefore, the question remains when exactly the micelles are adsorbed during the dipping process. To further clarify this issue, we have studied in some detail the role of the velocity at which the samples are removed from the micellar solution. It was found that for a given polymer concentration in solution there exists a typical withdrawing velocity v, at which an ordered array of micelles is observed after solvent evaporation. The result of this experiment is shown in Figure 6, where the value of the velocity v is shown as a function of polymer concentration in the solution. We find that the velocity needed for adsorption of a micellar layer increases as the polymer concentration is decreased.

The result shown in Figure 6 can be used to quantitatively check the notion of micelle adsorption as the relevant process of structure formation. Given that the pulling speed is large enough for the solution to wet the substrate at all, one can estimate the thickness of the liquid film after pulling and prior to solvent evaporation. Let γ and η be the surface tension and the viscosity of the solution, respectively. In the present situation $\eta v/\gamma << 1$ and one finds for the thickness h of a film adsorbed after pulling perpendicular to the surface of the solution reservoir[26]

$$h = 0.94\frac{(\eta v)^{2/3}}{(\rho g)^{1/2}\gamma^{1/6}}\left\{1 - 0.29\left(\frac{\eta v}{\gamma}\right)^{1/3}\right\} \qquad (10)$$

Here, ρ and g denote the density of the solution and the constant of gravity, respectively. For a given polymer concentration, we can use eq 10 to calculate the velocity v necessary to obtain a film of thickness h

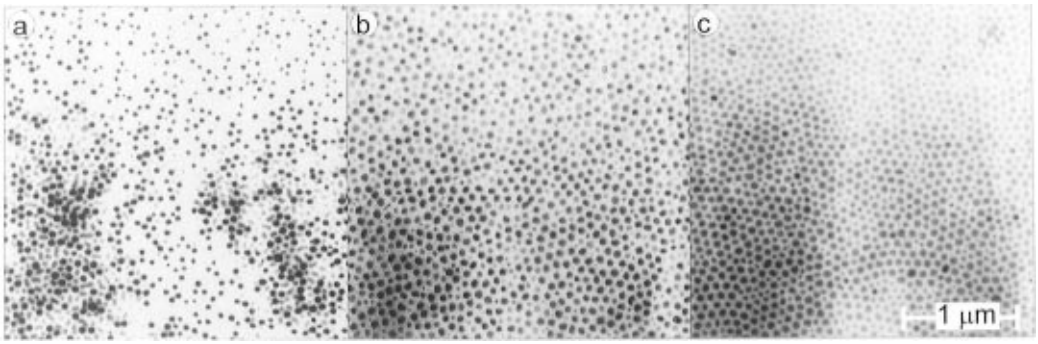

Figure 5. TEM image of micellar films drawn from a mixture of $CoCl_2$-labeled and unlabeled 1.5 mg/mL P(S-*b*-2VP) solutions ($M_{W(PS)}/M_{W(PVP)}$ = 84K/91K). Sample (a) was drawn immediately after the solutions were mixed, (b) was drawn 2 min later, and (c) was drawn 10 min after mixing.

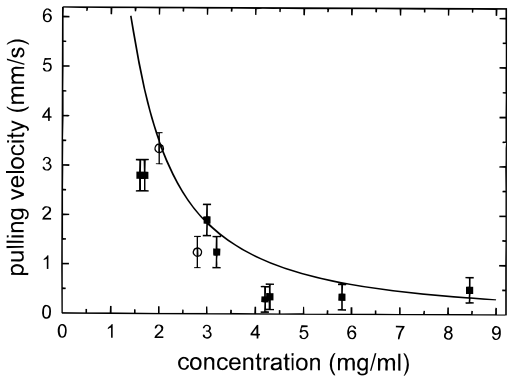

Figure 6. Typical pulling velocity for the deposition of a closed packed micellar film as a function of the concentration of the block copolymer solution. (■) $M_{W(PS)}/M_{W(PVP)}$ = 20K/120K, (○) $M_{W(PS)}/M_{W(PVP)}$ = 84K/91K.

which contains enough polymer to form a closed packed hexagonal lattice of micelles. We use the aggregation numbers and hydrodynamic radii obtained in sections III.1 and III.2 to calculate the solution viscosity according to the Einstein relation and obtain the solid line shown in Figure 6 together with the experimental data. Given that there is not an adjustable parameter in the calculation, the agreement is quite striking. The fact that the theoretical curve is shifted to somewhat higher velocities can easily be attributed to the fact that the micellar structures do not show perfect hexagonal packing. Therefore, the number of micelles is always smaller than theoretically assumed. In consequence, a smaller velocity is needed during the adsorption experiment.

We note that the experimental situation is somewhat more complex than suggested by eq 10. If we lower the pulling speed significantly below the values shown in Figure 6, we observe a discontinuous transition into a regime where no micelles are adsorbed at all. In particular for high polymer concentrations, one can reproducibly flip between the two regimes, i.e., the micellar structure observed after a fast enough pull is lost completely after reimmersing the sample and drawing slowly. A subsequent dipping and withdrawing at high enough velocity will then restore the original structure. A possible explanation for this finding is that at sufficiently low pulling velocities, there is enough time for the micellar layer to be "squeezed out" of the thin film wetting the substrate. Such a mechanism resembles what was recently observed by Krichevsky and Stavans,[27] who studied the thinning of soap films drawn from concentrated surfactant solutions. The authors observed a stepwise thinning of the soap film as a function of time after drawing. This effect is due to a layered organization of micelles in the highly confined geometry of the thin film. The experiments discussed in the present paper may similarly constitute a transition between a single layer and no layer of micelles. Since the micellar structures are rapidly frozen in after solvent evaporation, it is the velocity of pulling rather than the time after pulling which determines the final structure of the film.

IV. Conclusions

Summarizing the experimental results discussed above, a rather simple mechanism seems to be responsible for the formation of the micellar structures observed on surfaces dipped into a solution of diblock copolymer in a selective solvent. The aggregation numbers of micelles in solution as determined from dynamic light scattering compared well with aggregation numbers estimated from AFM measurements after solvent evaporation. This finding led to the assumption that entire micelles are adsorbed onto the sample surface. Adsorption experiments using mixtures of labeled and pure micelles strongly corroborated this assumption. Surface plasmon spectroscopy experiments indicated that in solution a brush of copolymer is formed on a polar substrate, while micelle adsorption happens only after removal of the sample from the solution. Experiments with varying drawing velocities confirmed this notion.

We note that our conclusion is in some contradiction to earlier work on the same polymers reported in ref 11. Within the estimated error, the AFM results on the symmetric copolymer are in agreement with the ones presented in ref 11, where the distance between protrusions was reported to be 100 nm, while the height was estimated as 8 nm. Assuming a spherical cap, one finds a volume of 3.1×10^{-17} cm^3 per protrusion corresponding to some 119 chains per microdomain. However, the light scattering data shown in the present study strongly disagree with an aggregation number as small as six chains per micelle as reported by Li *et al.*[11] Even a conservative estimate of the errors involved in calculating the aggregation numbers seems to rule out such a small number. It was, however, the difference between the small aggregation number obtained from light scattering and the larger aggregation number obtained from AFM measurements that led the authors of ref 11 to the conclusion that the ordered morphologies *cannot* be due to the adsorption of entire micelles. Aside from this difference, however, the experimental evidence of ref 11 can as well be understood assuming entire micelles to be adsorbed during solvent evaporation. In turn, we do not see how the results obtained on mixtures of $CoCl_2$-labeled and pure copolymer micelles (section

III.4) could be explained assuming a complex chain rearrangement near the surface during adsorption.

In conclusion, the experimental evidence presented in this paper strongly suggests that the formation of ordered two-dimensional structures observed after adsorption of P(S-*b*-2VP) block copolymers from a selective solvent can simply be explained by precipitation of micelles from the solution. It remains to be shown that the formation of wormlike micelles[6] observed at elevated temperatures and increased polymer concentrations follows a similar route. For this end, the dynamic light scattering experiments need to be extended to higher concentrations and elevated temperatures. This is the subject of ongoing work and shall be presented in a forthcoming publication.

Acknowledgment. We have benefitted from helpful discussions with U. Steiner. We are indebted to P. Leiderer for his help setting up the surface plasmon experiments and to R. Deike and F. Bitzer for their help during the dynamic light scattering experiments. We thank W. Rathmayer for providing the electron microscope. We are grateful to E. J. Kramer and his coworkers, who synthesized and characterized the copolymers used in this study. This work was made possible through the generous financial funding of the NATO, the Deutsche Forschungsgemeinschaft, and the Studienstiftung des Deutschen Volkes.

References and Notes

(1) For a recent review, see: Krausch, G. *Mat. Sci. Eng. Rep.* **1995**, *14*, 1 and references therein.
(2) Anastasiadis, S. H.; Russell, T. P.; Satija, S. K.; Majkrzak, C. F. *Phys. Rev. Lett.* **1989**, *62*, 1852.
(3) de Jeu, W. H.; Lambooy, P.; Hamley, I. W.; Vakin, D.; Pedersen, J. S.; Kjaer, K.; Seyger, R.; van Hutten, P.; Hadziioannou, G. *J. Phys. II (France)* **1993**, *3*, 139.
(4) Liu, Y.; Zhao, W.; Zheng, X.; King, A.; Sing, A.; Rafailovich, M. H.; Sokolov, J.; Dai, K. H.; Kramer, E. J.; Schwarz, S. A.; Sinha, S. K. *Macromolecules* **1994**, *27*, 4000.
(5) Spatz, J. P.; Sheiko, S.; Möller, M. *Adv. Mater.* **1996**, *8*, 513.
(6) Meiners, J. C.; Ritzi, A.; Rafailovich, M. H.; Sokolov, J.; Mlynek, J.; Krausch, G. *Appl. Phys.* **1995**, *A61*, 519.
(7) Spatz, J. P.; Roescher, A.; Sheiko, S.; Krausch, G.; Möller, M. *Adv. Mater.* **1995**, *7*, 731.
(8) Spatz, J. P.; Sheiko, S.; Möller, M. *Macromolecules* **1996**, *29*, 3220.
(9) Spatz, J. P.; Roescher, A.; Möller, M. *Adv. Mater.* **1996**, *8*, 337.
(10) Meiners, J. C.; Elbs, H.; Mlynek, J.; Krausch, G. *J. Appl. Phys.* **1996**, *80*, 2224.
(11) Li, Z.; Zhao, W.; Rafailovich, M. H.; Sokolov, J.; Khougaz, K.; Lennox, B.; Eisenberg, A.; Krausch, G. *J. Am. Chem. Soc.* **1996**, *118*, 10892.
(12) Synthesis and characterization of the block copolymers was performed by E. J. Kramer and co-workers, Dept. Materials Science and Engineering, Cornell University, Ithaca, NY 14850.
(13) We note that the height of the protrusions is not equivalent to the amplitude of the hight modulation observed on a regular structure such as the one shown in Figure 1. We rather use isolated protrusions (observed at lower polymer concentrations) for an accurate height determination.
(14) Tassin, J. F.; Siemens, R. L.; Tang, W. T.; Hadziioannou, G.; Swalen, J. D.; Smith, B. A. *J. Phys. Chem.* **1989**, *93*, 2106.
(15) Marques, C.; Joanny, J. F.; Leibler, L. *Macromolecules* **1988**, *21*, 1051.
(16) Daoud, M.; Cotton, J. P.; Farnoux, B.; Jannink, G.; Sarma, G.; Benoit, H.; Dupplessix, R.; Picot, C.; de Gennes, G. P. *Macromolecules* **1975**, *8*, 804.
(17) Daoud, M.; Cotton, J. P. *J. Phys.* **1982**, *43*, 531.
(18) Bug, A. L. R.; Cates, M. E.; Safran, S. A.; Witten, T. A. *J. Chem. Phys.* **1987**, *87*, 1824.
(19) Tuzar, Z.; Petrus, V.; Kratochvìl, P. *Makromol. Chem.* **1974**, *175*, 3181.
(20) Plestil, J.; Baldrián, J. *Makromol. Chem.* **1973**, *174*, 183.
(21) Cunham, P. A.; Lally, T. P.; Price, C.; Stubbersfield, R. B. *J. Chem. Soc., Faraday Trans. 1*, **1980**, *76*, 1857.
(22) Hipp, M.; Bielefeldt, H.; Colchero, J.; Marti, O.; Mlynek, J. *Ultramicroscopy* **1992**, *42*, 1498.
(23) Haziioannou, G.; Patel, S.; Granick, S.; Tirrell, M. *J. Am. Chem. Soc.* **1986**, *108*, 2869.
(24) Kaneko, M.; Tsuchida, E. *J. Polym. Sci.* **1982**, *16*, 397 and references herein.
(25) This assumption is corroborated by AFM investigations comparing films adsorbed from nonlabeled copolymer solutions and those adsorbed from $CoCl_2$-labeled copolymer solutions. We were not able to detect any significant influence of the metal salt on the resulting structures in the adsorbed films.
(26) Deryagin, B. M.; Levi, S. M. *Film Coating Theory*; The Focal Press: London, 1964.
(27) Krichevsky, O.; Stavans, J. *Phys. Rev. Lett.* **1995**, *74*, 2752.
(28) We find $\sigma = 0.0044$ in good agreement with: Parsonage, E.; Tirrell, M.; Watanabe, H.; Nuzzo, R. G. *Macromolecules* **1991**, *24*, 1987.

MA970327T